11

Controlled defect mode suppression in a photonic crystal with graphene particles

© I.A. Glukhov[1,2], S.G. Moiseev[1,2]

[1] Ulyanovsk State University,
Ulyanovsk, Russia
[2] Kotelnikov Institute of Radio Engineering and Electronics of the Russian Academy of Sciences, Ulyanovsk Branch,
Ulyanovsk, Russia

e-mail: glukhov91@yandex.ru

Received April 29, 2025
Revised September 10, 2025
Accepted October 24, 2025

The transmission spectra in the terahertz frequency range of a one-dimensional photonic crystal structure with ordered layers of graphene particles placed in a defect layer are studied. Graphene particles and graphene wires connecting them form two-dimensional arrays whose chemical potential can be varied by the magnitude of applied electric potential. The possibility of controlling the transmission coefficient in the mini-zone associated with the defect mode of the photonic crystal in the range of 0.05−0.7 is shown.

Keywords: photonic crystal, microresonator, graphene particles, transmission spectrum, tuning.

DOI: 10.61011/EOS.2025.10.62560.8058-25

Introduction

Further development of photonics requires the development and improvement of structures for controlling, localizing, and absorbing electromagnetic radiation in the terahertz frequency range. Solving these problems is necessary, among other things, for developing sensors and radiation energy converters. Structured materials and layered periodic structures find application to enhance the efficiency of radiation capture and absorption [1,2]. In photonic crystal microcavities, enhancement of the interaction between radiation and the material or low-dimensional structures can be achieved in a relatively narrow spectral mini-band within the photonic bandgap [3,4]. The use of graphene monolayers in such structures, whose optical properties depend on variable external factors (electric and magnetic fields, temperature, etc.), enables tunable reconfiguration of transmission and reflection spectra [5,6].

At present, a technology for fabricating microstructured graphene has been developed, allowing the production of graphene particles (fragments of a graphene monolayer) with controlled shape and size [7]. Such graphene structures efficiently interact with electromagnetic radiation at frequencies of localized plasmon resonance in the terahertz domain [8–10]. In this work, the parameters of two-dimensional arrays of graphene particles (GPs) are determined; their incorporation into a microcavity enables control of the transmission spectrum in the photonic bandgap by varying the applied potential difference.

Geometry of the Structure. Control of Transmission in the Photonic Structure at the Defect Mode Frequency

The structure under consideration is a one-dimensional resonator consisting of two dielectric mirrors and a dielectric layer in which GPs are placed (Fig. 1). The dielectric mirrors are formed by N alternating layers A and B of non-absorbing materials with refractive indices n_A, n_B and thicknesses d_A, d_B satisfying the Bragg resonant reflection condition at frequency ν_{Br}: $d_A n_A = d_B n_B = c/4\nu_{Br}$, where c is the speed of the electromagnetic wave in vacuum. The defect layer D, serving as the resonant cavity, is made of a non-absorbing material with refractive index n_D has a thickness of $d_D = c/n_D\nu_{Br}$. For the chosen parameters, a narrow transmission line exists in the photonic bandgap, associated with the defect mode at frequency ν_{Br}. Each GP represents a subwavelength-sized fragment of a graphene monolayer. The GPs have identical shape and size, are similarly oriented in the plane xOy and form a two-dimensional (2D) array. To control the chemical potential (Fermi energy) of the GPs, they are electrically connected into a continuous array by graphene strips — graphene wires (schematically shown in the pictogram at the bottom of Fig. 1).

It is assumed that the GPs generally have an elliptical shape and are positioned at the nodes of a lattice with a square unit cell and period p. The ellipse is characterized by the aspect ratio $\xi = a/b$, where a and b are the lengths of its semi-axes along the coordinate axes x and y respectively. By varying the aspect ratio, particles of different shapes can be modeled: $\xi = 1$ corresponds to a circle, $\xi > 1$ ($\xi < 1$) — to an elongated (compressed)

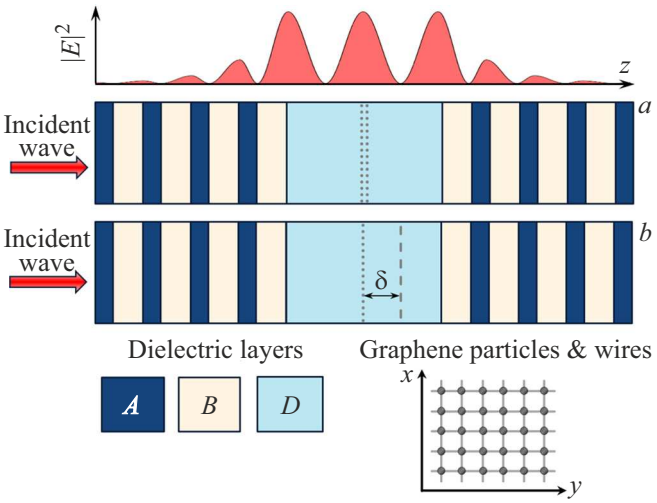

Figure 1. Dielectric layers A, B and D form a one-dimensional photonic structure $[AB]^N D[BA]^N$. In layer (a) two GP arrays (dotted lines) or (b) one GP array (dotted line) and a solid graphene layer (dashed line) are placed at a distance δ from each other. The upper part of the figure shows the intensity distribution of the optical field (in relative units) across the photonic structure (without GPs and graphene) at the defect mode frequency. The bottom part of the figure illustrates the structure of the 2D GP array.

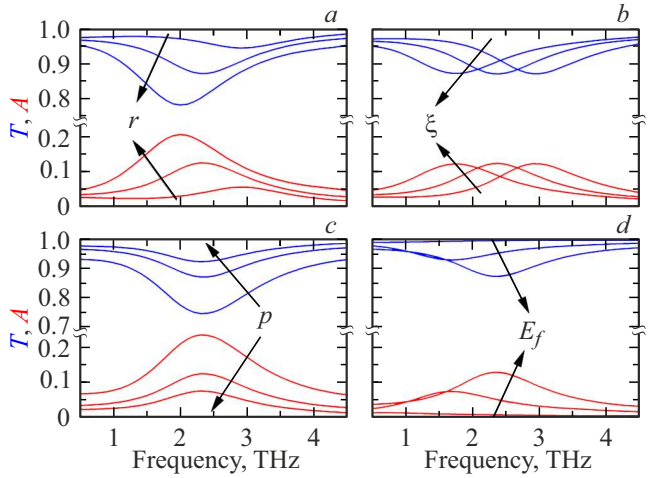

Figure 2. Dependence of absorption spectra (red curves) and transmission (blue curves) of a 2D GP array on (a) GP radius for circular shape $(a = b = r)$, (b) GP shape, (c) inter-particle distance, (d) GP Fermi energy. Arrows with labels on the plots indicate the direction of increasing respective parameter.

ellipse along the coordinate axis x. The electric field vector (plane of polarization) of the electromagnetic radiation propagating along the axis z coincides with the direction of the translation vectors of the particle array unit cell (i.e., aligned along the axis x or y). For circular GPs, the spectral characteristics of the structure are invariant under rotation of the polarization plane by an angle multiple of $\pi/2$.

Two configurations of the photonic structure are considered: one includes two closely spaced identical 2D GP arrays placed at the center of the microcavity (Fig. 1, a), the other — a single 2D GP array at the center of the microcavity and a graphene layer at a distance $\delta = \lambda_{Br}/4n_d$ from it (Fig. 1, b). The presence of a pair of two-dimensional graphene structures in each case („GP array + GP array“ or „GP array + graphene“) allows controlled variation of the Fermi energy of the GPs via the applied potential difference.

Note that for both configurations, at the defect mode frequency of the photonic structure, the GP arrays are located in the region of optical field localization (see the $|E|^2(z)$ plot in Fig. 1), which maximizes the efficiency of their interaction with electromagnetic radiation. In the case shown in Fig. 1, b, the graphene layer serving as the second electrode is situated in a region of nearly zero optical field intensity (in the „electromagnetic shadow“) and, consequently, does not significantly affect the defect mode amplitude.

In this work, the spectral characteristics of 2D GP arrays and photonic structures of the two configurations were calculated using numerical modeling implemented in the COMSOL Multiphysics software package. The computational model employs the surface current method, enabling the modeling of graphene structures, including GP arrays and interconnecting graphene wires, as infinitely thin structured layers; their electrodynamic properties are described by specifying the graphene surface conductivity. The graphene surface conductivity is calculated using the Kubo formula:

$$\sigma_S(\nu) = \sigma_S^{intra}(\nu) + \sigma_S^{inter}(\nu) = \frac{2e^2 k_B T}{\pi\hbar^2} \times \ln\left(2\cosh\frac{E_F}{2k_B T}\right)\frac{i}{2\pi\nu + i/\tau} + \frac{e^2}{4\hbar}\left[H(\pi\nu) + i2\nu\int_0^{+\infty}\frac{H(\Omega) - H(\pi\nu)}{(\pi\nu)^2 - \Omega^2}\,d\Omega\right],$$

where

$$H(\Omega) = \sinh(\hbar\Omega/k_B T)/\left(\cosh(\hbar\Omega/k_B T) + \cosh(E_F/k_B T)\right),$$

E_F is Fermi energy, T is temperature $(T = 300\,\mathrm{K})$, ν is electromagnetic wave frequency, τ is relaxation time $(\tau = 10^{-13}\,\mathrm{s})$ [8].

To illustrate the optical characteristics of a 2D GP array, Fig. 2 presents the results of electrodynamic modeling for the case where the array is embedded in an infinite medium TOPAS (polyethylene cyclic olefin copolymer) with refractive index $n_D = 1.6$ [10]. The width of the graphene conductors is $0.5\,\mu$m. The GP array parameters are given in the table. The plots show that the frequency dependence of absorption and transmission exhibits a resonant character. The most pronounced changes in spectral characteristics occur at the frequency of the localized

Parameters of the GP array in Fig. 2, $a-d$

Fig. 2	a, μm	ξ	p, μm	E_F, eV
a	4, 6, 8	1	30	0.5
b	6	0.5, 1, 2	30	0.5
c	6	1	20, 30, 40	0.5
d	6	1	30	0, 0.25, 0.5

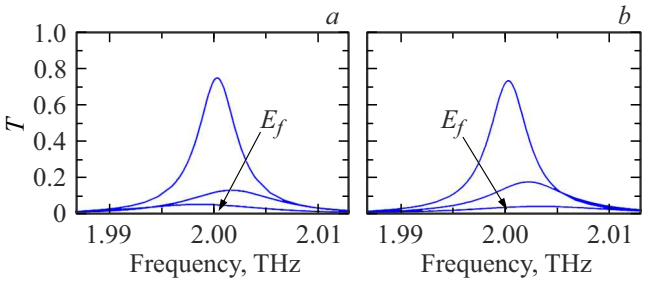

Figure 3. Transmission spectrum for a photonic crystal microcavity with a double GP array (a), or GP array and graphene layer (b). GP array parameters: $a = b = 10\,\mu$m ($\xi = 1$), $p = 120\,\mu$m (a), $80\,\mu$m (b). The Fermi energy of the graphene structures takes values of 0, 0.25, and 0.5 eV. Arrows indicate the directions of increasing Fermi energy.

surface plasmon resonance of the GPs, which depends on the GP size (Fig. 2, a) and shape (Fig. 2, b). As the inter-particle distance p increases, the fraction of absorbed energy decreases (Fig. 2, c). The absorption capacity of the GP array can be varied by changing the applied potential difference (Fig. 2, d).

The dependence of the GP array absorptivity on its geometric parameters and applied potential difference allows matching the GPs and dielectric layer parameters of the photonic structure to enable control of transmitted radiation intensity at the defect mode frequency. As seen from Fig. 3, for the proposed microcavity configurations, varying the GP Fermi energy from 0 to 0.5 eV changes the transmission from 0.05 to 0.7. The photonic structure is formed by dielectric mirrors with $N = 4$ layer pairs of Si and SiO_2 with refractive indices $n_A = 3.42$ and $n_B = 1.96$ respectively [11]. The dielectric layer thicknesses satisfy the Bragg resonant reflection condition at frequency $\nu_{Br} = 2$ THz. Two-dimensional arrays of circular GPs are placed at the center of layer D, made of TOPAS. The graphene conductor width is $0.5\,\mu$m. For the two GP arrays case (Fig. 3, a), the distance between them is 1 nm. In the structure with one GP array (Fig. 3, b), the solid graphene layer is placed at a distance $\delta = \lambda_{Br}/4n_d = 23.4\,\mu$m from the GPs. The potential differences required to achieve the maximum Fermi energy (0.5 eV) applied to the graphene conductors are 2.4 V and 55 kV in these schemes. The higher voltage (up to 55 kV) is required in the scheme with electrodes separated by $\delta = 23.4\,\mu$m (the case shown in Fig. 3, b).

The results of electrodynamic modeling presented in Fig. 3, a and Fig. 3, b were obtained for the cases where absorption occurs in the double and single GP arrays, respectively (in the second configuration, graphene sheet interacts negligibly with electromagnetic radiation). For identical array parameters, the scattering intensity and energy dissipation in the single GP array are lower; however, as seen from the plots, its influence on the defect mode can be enhanced by denser particle placement. It should be noted that for both configurations, at any Fermi energy value, the difference between the maximum and minimum values of the energy transmission coefficient T is less than one due to radiation absorption by the GPs and graphene wires.

Conclusion

This work proposes a design for a photonic crystal microcavity incorporating two-dimensional arrays of micrometer-sized GPs, whose transmission coefficient at the defect mode frequency is controlled by the applied potential difference. Transmission control is achieved through the dependence of the GP absorption coefficient on the applied potential difference. High efficiency in radiation energy capture and absorption is attained by matching the position of the GP array and frequency of the GP localized plasmon resonance with the field localization region and frequency of the microcavity photonic mode. It is demonstrated that such terahertz radiation modulators can be implemented using just one (Fig. 1, b) or two (Fig. 1, a) two-dimensional GP arrays. The transmission coefficient in both schemes can be controllably varied from 0.05 to 0.7.

It should be noted that the dependence of the GP array resonance frequency on its structural parameters enables bandwidth control at other operating frequencies (within the microcavity photonic bandgap). Using similar modulator schemes with graphene layers of alternative designs, control of electromagnetic wave polarization state can also be realized.

Funding

The work was carried out within the framework of the state task of the Ministry of Science and Higher Education of the Russian Federation (FEUF-2023-0003).

Conflict of interest

The authors declare that they have no conflict of interest.

References

[1] R. Kakimi, M. Fujita, M. Nagai, M. Ashida, T. Nagatsuma. Nature Photon, **8**, 657 (2014). DOI: 10.1038/nphoton.2014.150

[2] A. Mokhtari, M.H. Rezaei, A. Zarifkar. App. Opt., **62**, 3660 (2023). DOI: 10.1364/AO.484617

[3] I.V. Timofeev, D.N. Maksimov, A.F. Sadreev. Phys. Rev. B, **97**, 024306 (2018). DOI: 10.1103/PhysRevB.97.024306
[4] I.A. Glukhov, Y.S. Dadoenkova, F.F.L. Bentivegna, S.G. Moiseev. J. App. Phys., **128** (5), 053101 (2020). DOI: 10.1063/5.0008652
[5] I.V. Fedorova, S.V. Eliseeva, D.I. Sementsov. App. Sci., **13** (13), 7559 (2023). DOI: 10.3390/app13137559
[6] A. Rashidi, A. Namdar. Opt. Quant. Electron., **50**, 279 (2018). DOI: 10.1007/s11082-018-1534-9
[7] M. Zeng, Y. Xiao, J. Liu, W. Lu, L. Fu. Adv. Electron. Mat., **2** (4), 1500456 (2016). DOI: 10.1002/aelm.201500456
[8] A. Andryieuski, A.V. Lavrinenko. Opt. Express, **21**, 9144–9155 (2013). DOI: 10.1364/OE.21.009144
[9] S. Thongrattanasiri, F.H.L. Koppens, F.J. García de Abajo. Phys. Rev. Lett., **108**, 047401 (2012). DOI: 10.1103/PhysRevLett.108.047401
[10] S. Yang, G. Wang, X. Zhang, J. Liu, M. Li, Y. Jia, H. Meng, Y. Gao. Opt. Mat., **154**, 115704 (2024). DOI: 10.1016/j.optmat.2024.115704
[11] E.D. Palik. *Handbook of Optical Constants of Solids*, Vol. 1 (Academic Press, 1998).

Translated by J.Savelyeva